

Geometric Correspondence Consistency in RGB-D Relative Pose Estimation

Supplementary Material

1. Notation Table

Symbol	Interpretation
Γ_i	A 3D point with index i
γ_i	A 2D point in meters with index i
ξ_i	x -coordinate of γ_i
η_i	y -coordinate of γ_i
ρ_i	Depth of the i th 3D point, $\Gamma_i = \rho_i \gamma_i$
\mathcal{R}	Rotation matrix
\mathcal{T}	Translation vector
$\bar{\Gamma}_i$	A 3D point Γ_i in another camera coordinate, related by $\bar{\Gamma}_i = \mathcal{R}\Gamma_i + \mathcal{T}$
$\bar{\gamma}_i$	A 2D point in correspondence with γ_i
$\bar{\rho}_i$	Depth of $\bar{\Gamma}_i$, $\bar{\Gamma}_i = \bar{\rho}_i \bar{\gamma}_i$
$\bar{\xi}_i$	x -coordinate of $\bar{\gamma}_i$
$\bar{\eta}_i$	y -coordinate of $\bar{\gamma}_i$
r	Distance of two 3D points, $r = \ \Gamma_i - \Gamma_j\ $
S	Scene surface
\hat{C}	A curve as the intersection of a sphere of radius r centered at Γ_i and the scene surface S
C	A 2D curve as a projection from \hat{C}
\bar{C}	A 2D curve corresponding to C
\bar{d}^*	The distance of $\bar{\gamma}$ from the curve \bar{C}
$\nabla \rho$	Gradient of depth ρ
Δ	Feature point location error

Table 8. Notations used in this paper.

2. Proof of Proposition 1

Proposition 1. Let r and \bar{r} be the radial maps of the first and second images, with respect to (γ_0, ρ_0) and $(\bar{\gamma}_0, \bar{\rho}_0)$, respectively. Given a putative correspondence, $(\gamma, \bar{\gamma})$, the first-order approximation of the level-set gives the distance \bar{d} of $\bar{\gamma}$ from the corresponding r -level-set as

$$\bar{d}^* = \frac{\bar{r}|r - \bar{r}|}{\left\| (\bar{\rho}\|\bar{\gamma}\|^2 - \bar{\rho}_0\bar{\gamma}_0^T\bar{\gamma})\nabla\bar{\rho} + \bar{\rho} \begin{bmatrix} \bar{\rho}\bar{\xi} - \bar{\rho}_0\bar{\xi}_0 \\ \bar{\rho}\bar{\eta} - \bar{\rho}_0\bar{\eta}_0 \end{bmatrix} \right\|}, \quad (13)$$

where $\bar{\rho}(\bar{\xi}, \bar{\eta})$ is the depth at $\bar{\gamma}(\bar{\xi}, \bar{\eta})$.

Proof. The true correspondence point, $\bar{\gamma}^*$, must lie on the corresponding curve to the curve γ lies on, Figure 5, *i.e.*, $\bar{r}(\bar{\gamma}^*) = r(\gamma)$. Thus, $\bar{\gamma}^*$ can be identified as any arbitrary point $\hat{\gamma}$ on the the r -level-set \bar{r} that has the least perturbation from the observed point $\bar{\gamma}$, *i.e.*,

$$\bar{d} = \min_{\hat{\gamma}, \bar{r}(\hat{\gamma})=r(\gamma)} d(\bar{\gamma}, \hat{\gamma}). \quad (14)$$

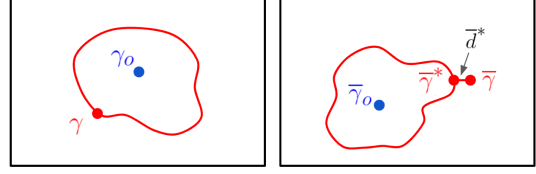


Figure 1. The geometric correspondence consistency constrains a correspondence (γ, ρ) and $(\bar{\gamma}, \bar{\rho})$ to lie on the corresponding curves with respect to a reference point correspondence (γ_0, ρ_0) and $(\bar{\gamma}_0, \bar{\rho}_0)$. Due to noise in feature location and depth measurement, the observed correspondence $\bar{\gamma}_i$ is a perturbation of the true corresponding point $\bar{\gamma}^*$ by \bar{d}^* .

Denoting $\gamma = (\xi, \eta)$, $\hat{\gamma} = (\hat{\xi}, \hat{\eta})$, and $\bar{\gamma} = (\bar{\xi}, \bar{\eta})$, this can be written as

$$\bar{d} = \min_{\hat{\gamma}, \bar{r}(\hat{\gamma})=r(\gamma)} \left[(\hat{\xi} - \bar{\xi})^2 + (\hat{\eta} - \bar{\eta})^2 \right]^{\frac{1}{2}}. \quad (15)$$

Now, since the perturbation of $\hat{\gamma}$ is small, a first-order approximation holds, *i.e.*,

$$\bar{r}(\hat{\xi}, \hat{\eta}) \cong \bar{r}(\bar{\xi}, \bar{\eta}) + \nabla \bar{r}(\bar{\xi}, \bar{\eta}) \begin{bmatrix} \hat{\xi} - \bar{\xi} \\ \hat{\eta} - \bar{\eta} \end{bmatrix}. \quad (16)$$

Using $\bar{r}(\hat{\xi}, \hat{\eta}) = r(\xi, \eta)$, this gives one equation in the unknown $(\hat{\xi}, \hat{\eta})$, so that $\hat{\eta}$ can be written in terms of $\hat{\xi}$ by solving

$$r(\xi, \eta) = \bar{r}(\bar{\xi}, \bar{\eta}) + \bar{r}_{\xi}(\bar{\xi}, \bar{\eta})(\hat{\xi} - \bar{\xi}) + \bar{r}_{\eta}(\bar{\xi}, \bar{\eta})(\hat{\eta} - \bar{\eta}). \quad (17)$$

This gives

$$(\hat{\eta} - \bar{\eta}) = \frac{r(\xi, \eta) - \bar{r}(\bar{\xi}, \bar{\eta}) - \bar{r}_{\xi}(\bar{\xi}, \bar{\eta})(\hat{\xi} - \bar{\xi})}{\bar{r}_{\eta}(\bar{\xi}, \bar{\eta})}. \quad (18)$$

Thus, the minimization over two variables in Equation 15 can be written over a single variable $\hat{\xi}$,

$$\begin{aligned} \bar{d} &= \arg \min_{\hat{\xi}} \left[(\hat{\xi} - \bar{\xi})^2 + \frac{r(\xi, \eta) - \bar{r}(\bar{\xi}, \bar{\eta}) - \bar{r}_{\xi}(\bar{\xi}, \bar{\eta})(\hat{\xi} - \bar{\xi})}{\bar{r}_{\eta}(\bar{\xi}, \bar{\eta})} \right]^{\frac{1}{2}} \\ &= \arg \min_{\hat{\xi}} \left[\left(1 + \frac{\bar{r}_{\xi}^2(\bar{\xi}, \bar{\eta})}{\bar{r}_{\eta}^2(\bar{\xi}, \bar{\eta})} \right)^2 (\hat{\xi} - \bar{\xi})^2 \right. \\ &\quad \left. - 2 \left(r(\xi, \eta) - \bar{r}(\bar{\xi}, \bar{\eta}) \right) \frac{\bar{r}_{\xi}(\bar{\xi}, \bar{\eta})}{\bar{r}_{\eta}^2(\bar{\xi}, \bar{\eta})} (\hat{\xi} - \bar{\xi}) \right. \\ &\quad \left. + \left(\frac{r(\xi, \eta) - \bar{r}(\bar{\xi}, \bar{\eta})}{\bar{r}_{\eta}(\bar{\xi}, \bar{\eta})} \right)^2 \right]^{\frac{1}{2}} \end{aligned} \quad (19)$$

Differentiating this equation with respect to $\hat{\xi}$ and setting to zero gives

$$\left(1 + \frac{\bar{r}_{\xi}^2(\bar{\xi}, \bar{\eta})}{\bar{r}_{\eta}^2(\bar{\xi}, \bar{\eta})}\right) (\hat{\xi} - \bar{\xi}) - (r(\xi, \eta) - \bar{r}(\bar{\xi}, \bar{\eta})) \frac{\bar{r}_{\xi}(\bar{\xi}, \bar{\eta})}{\bar{r}_{\eta}^2(\bar{\xi}, \bar{\eta})} = 0, \quad (20)$$

so that

$$\begin{aligned} (\hat{\xi} - \bar{\xi}) &= \frac{(r(\xi, \eta) - \bar{r}(\bar{\xi}, \bar{\eta})) \bar{r}_{\xi}(\bar{\xi}, \bar{\eta})}{\bar{r}_{\xi}^2(\bar{\xi}, \bar{\eta}) + \bar{r}_{\eta}^2(\bar{\xi}, \bar{\eta})} \\ &= \frac{r(\xi, \eta) - \bar{r}(\bar{\xi}, \bar{\eta})}{\|\nabla \bar{r}\|^2(\bar{\xi}, \bar{\eta})} \bar{r}_{\xi}(\bar{\xi}, \bar{\eta}). \end{aligned} \quad (21)$$

Similarly,

$$(\hat{\eta} - \bar{\eta}) = \frac{r(\xi, \eta) - \bar{r}(\bar{\xi}, \bar{\eta})}{\|\nabla \bar{r}\|^2(\bar{\xi}, \bar{\eta})} \bar{r}_{\eta}(\bar{\xi}, \bar{\eta}). \quad (22)$$

Thus, the optimal distance \bar{d} is,

$$\begin{aligned} \bar{d} &= \left[(\hat{\xi} - \bar{\xi})^2 + (\hat{\eta} - \bar{\eta})^2 \right]^{\frac{1}{2}} = \left[\frac{(r(\xi, \eta) - \bar{r}(\bar{\xi}, \bar{\eta}))^2}{\|\nabla \bar{r}\|^2(\bar{\xi}, \bar{\eta})} \right]^{\frac{1}{2}} \\ &= \frac{|r(\xi, \eta) - \bar{r}(\bar{\xi}, \bar{\eta})|}{\|\nabla \bar{r}\|(\bar{\xi}, \bar{\eta})}. \end{aligned} \quad (23)$$

Now, this expression can be reduced to gradient of ρ which is directly available, since by definition,

$$\begin{aligned} \bar{r}(\hat{\xi}, \hat{\eta}) &= \left\| \hat{\rho}(\hat{\xi}, \hat{\eta}) \hat{\gamma}(\hat{\xi}, \hat{\eta}) - \rho_0 \gamma_0 \right\| \\ &= \left[(\hat{\rho} \hat{\xi} - \bar{\rho}_0 \bar{\xi}_0)^2 + (\hat{\rho} \hat{\eta} - \bar{\rho}_0 \bar{\eta}_0)^2 + (\hat{\rho} - \bar{\rho}_0)^2 \right]^{\frac{1}{2}}. \end{aligned} \quad (24)$$

The gradient $\nabla \bar{r}$ can be written in terms of $\nabla \hat{\rho}$,

$$\begin{aligned} \nabla \bar{r}(\hat{\xi}, \hat{\eta}) &= \frac{1}{2} \left(\frac{2(\hat{\rho} \hat{\xi} - \bar{\rho}_0 \bar{\xi}_0)(\nabla \hat{\rho} \hat{\xi} + \hat{\rho} e_1) + 2(\hat{\rho} \hat{\eta} - \bar{\rho}_0 \bar{\eta}_0)(\nabla \hat{\rho} \hat{\eta} + \hat{\rho} e_2) + 2(\hat{\rho} - \bar{\rho}_0) \nabla \hat{\rho}}{\left((\hat{\rho} \hat{\xi} - \bar{\rho}_0 \bar{\xi}_0)^2 + (\hat{\rho} \hat{\eta} - \bar{\rho}_0 \bar{\eta}_0)^2 + (\hat{\rho} - \bar{\rho}_0)^2 \right)^{\frac{1}{2}}} \right) \\ &= \frac{1}{\bar{r}(\hat{\xi}, \hat{\eta})} \left(\left((\hat{\rho} \hat{\xi} - \bar{\rho}_0 \bar{\xi}_0) \hat{\xi} + (\hat{\rho} \hat{\eta} - \bar{\rho}_0 \bar{\eta}_0) \hat{\eta} + (\hat{\rho} - \bar{\rho}_0) \right) \nabla \hat{\rho} \right. \\ &\quad \left. + \hat{\rho} \begin{bmatrix} \hat{\rho} \hat{\xi} - \bar{\rho}_0 \bar{\xi}_0 \\ \hat{\rho} \hat{\eta} - \bar{\rho}_0 \bar{\eta}_0 \end{bmatrix} \right) \\ &= \frac{1}{\bar{r}(\hat{\xi}, \hat{\eta})} \left[(\hat{\rho} \|\hat{\gamma}\|^2 - \bar{\rho}_0 \bar{\gamma}_0^T \hat{\gamma}) \nabla \hat{\rho} + \hat{\rho} \begin{bmatrix} 1 & 0 & 0 \\ 0 & 1 & 0 \end{bmatrix} (\hat{\rho} \hat{\gamma} - \bar{\rho}_0 \bar{\gamma}_0) \right]. \end{aligned} \quad (25)$$

Using this expression in Equation 23 at $(\bar{\xi}, \bar{\eta})$ gives,

$$\begin{aligned} \bar{d}^* &= \frac{|r(\xi, \eta) - \bar{r}(\bar{\xi}, \bar{\eta})|}{\|\nabla \bar{r}\|(\bar{\xi}, \bar{\eta})} \\ &= \frac{\bar{r}(\bar{\xi}, \bar{\eta}) |r(\xi, \eta) - \bar{r}(\bar{\xi}, \bar{\eta})|}{\left\| (\bar{\rho} \|\bar{\gamma}\|^2 - \bar{\rho}_0 \bar{\gamma}_0^T \bar{\gamma}) \nabla \bar{\rho} + \bar{\rho} \begin{bmatrix} 1 & 0 & 0 \\ 0 & 1 & 0 \end{bmatrix} (\bar{\rho} \bar{\gamma} - \bar{\rho}_0 \bar{\gamma}_0) \right\|}. \end{aligned} \quad (26)$$

3. Time Savings from the GCC-filtered RANSAC Contributed to Increased Accuracy

Table 1 in the main manuscript outlines the average cost associated with evaluating hypotheses, highlighting that the primary computational expense is attributed to measuring hypothesis support. The application of geometric correspondence constraints to all pairs of triplet correspondences

Sequence	Metrics	Narrow 1-frame	7-frame apart	14-frame apart	22-frame apart	Wide 30-frame
		Classic / GCC-Filtered	Classic / GCC-Filtered	Classic / GCC-Filtered	Classic / GCC-Filtered	Classic / GCC-Filtered
fr1/desk	RPE _{trans} (cm)	1.14 / 0.9	5.85 / 3.01	7.90 / 4.23	48.89 / 4.16	81.41 / 7.02
	RPE _{rot} (degree)	0.56 / 0.5	0.67 / 0.65	4.46 / 0.79	40.92 / 0.80	68.00 / 1.02
fr1/room	RPE _{trans} (cm)	0.77 / 0.69	17.85 / 4.38	66.29 / 5.70	137.54 / 6.3	157.41 / 8.80
	RPE _{rot} (degree)	0.41 / 0.36	13.55 / 1.18	26.57 / 2.60	68.52 / 3.40	89.10 / 6.10
fr1/xyz	RPE _{trans} (cm)	0.53 / 0.49	1.30 / 1.00	1.90 / 1.41	34.32 / 3.24	38 / 3.8
	RPE _{rot} (degree)	0.32 / 0.36	0.67 / 0.62	0.94 / 0.82	34.23 / 1.8	40.62 / 2.7
fr2/desk	RPE _{trans} (cm)	2.62 / 0.89	6.9 / 2.47	9.81 / 3.56	34.32 / 4.39	14.41 / 4.97
	RPE _{rot} (degree)	0.72 / 0.49	6.4 / 2.3	9.79 / 3.49	12.9 / 4.22	13.6 / 5.1
fr3/struct	RPE _{trans} (cm)	1.21 / 0.99	1.4 / 1.01	1.53 / 1.02	1.53 / 1.07	1.96 / 1.4
	RPE _{rot} (degree)	0.81 / 0.60	0.81 / 0.73	0.87 / 0.77	0.90 / 0.8	1.03 / 0.9
fr3/office	RPE _{trans} (cm)	0.57 / 0.45	0.83 / 0.75	1.09 / 0.77	1.30 / 0.81	1.88 / 0.9
	RPE _{rot} (degree)	0.69 / 0.24	0.51 / 0.3	0.75 / 0.32	0.81 / 0.38	0.87 / 0.41
Number of Iterations		3000 / 7795	3000 / 8891	3000 / 12112	3000 / 14832	3000 / 16132
Execution Time (s)		0.13	0.13	0.13	0.13	0.13

Table 9. Pose estimation errors RPE_{trans} (cm) and RPE_{rot} (degree) classic RANSAC (**Classic**) and GCC-filtered RANSAC (**GCC-Filtered**) across different baselines, keeping equal execution time.

that formulate a hypothesis significantly reduces the pool of viable hypotheses. This reduction leads to an increase in the cost of hypothesis formulation, denoted as α , but results in savings in the cost of measuring hypothesis support, denoted as β , since only a fraction μ of N is computed. Consequently, the total computational cost is expressed as $N(\alpha + \mu\beta)$. Although the cost α escalates from $0.96\mu s$ to approximately $1.69\mu s$, the reduction factor μ markedly decreases the overall cost. It is important to note that μ varies with the outlier ratio; scenarios with wider baselines and higher outlier counts see more pronounced speed improvements as fewer hypotheses meet the constraints, thereby reducing the cost of inlier support measurement.

In Table 9, the last two rows, where different baseline performances are compared, the classic RANSAC algorithm undergoes 3000 iterations, and the execution time which is 0.138 seconds is fixed in this experiment. Under these conditions, the number of iterations performed by GCC-filtered RANSAC varies with the baseline distance: 7795 iterations for a narrow baseline (1-frame apart), 8891 iterations for 7-frame apart, 12112 iterations for 14-frame apart, 14832 iterations for 22-frame apart, and 16132 iterations for a wide baseline of 30 frames apart. These iterations are average of all image pairs withing each baseline category. Evidently, the results demonstrate that GCC enables a higher number of iterations within the same time frame, contributing to enhanced accuracy.